ISSN 1068–3372, Journal of Contemporary Physics (Armenian Academy of Sciences), 2019, Vol. 54, No. 2, pp. 146–152. © Allerton Press, Inc., 2019.
Russian Text © The Author(s), 2019, published in Izvestiya Natsional'noi Akademii Nauk Armenii, Fizika, 2019, Vol. 54, No. 2, pp. 198–205.

Current Transport Mechanism in p-InSb–n-CdTe Heterojunction

S. G. Petrosyan[a,b], L. M. Matevosyan[a,b], K. E. Avjyan[a,b*], and S. R. Nersesyan[b]

[a]*Russian–Armenian University, Yerevan, Armenia*
[b]*Institute of Radiophysics and Electronics, NAS of Armenia, Ashtarak, Armenia*
[*]*avjyan@gmail.com*

Received November 30, 2018

Abstract—Based on the analysis of the forward current-voltage characteristics of the p-InSb–n-CdTe heterojunction fabricated by a method of pulsed laser deposition, the existence of two charge injection mechanisms was experimentally confirmed. At relatively small external bias voltages (0.03 V < U < 0.15 V), the current is in a satisfactory agreement with the expression $I \sim \exp(qU/\eta kT)$ with the ideality factor $\eta = 1$. Above 0.18 V, the current-voltage characteristic obeys the law $I \sim U^{3/2}$ followed by an attainment to the linear section (the cut-off voltage of current is 0.47 V). A theoretical model of current transport is given taking into account the peculiarities of the heterojunction band discontinuity, leading to the origination of inversion layer near the interface.

DOI: 10.3103/S1068337219020051
Keywords: heterojunction, pulsed laser deposition, current transport mechanism

1. INTRODUCTION

The creation of devices for the generation and reception of electromagnetic radiation of the infrared (IR) range is dictated by the wide use of receiving and transmitting devices of this range to solve the important tasks, such as the monitoring of atmosphere, diagnosing damage to gas and oil pipelines, thermal imaging with increased temperature contrast, wireless optical communication, the detection of thermal objects and other.

Using a simple low-temperature pulsed laser deposition technology (excluding implantation processes, the high-temperature diffusion and annealing), we fabricated previously the p-InSb–n-CdTe heterojunction (HJ) photoreceivers sensitive in the optical range of 1–5.8 μm [1–3]. It is shown, in particular, that such single photodetectors can have an integral sensitivity not lesser than 1000 mV/mW, a photoresponse time of about 15 ns, a detecting ability of about 1.8×10^{11} cm Hz$^{1/2}$ W^{-1} at a wavelength of 4.8 μm. By these parameters, they are not inferior to traditional photodetectors based on the InSb [4]. We also showed that it is possible to determine the spatial position and parameters of motion of various objects emitting in the IR range [5] with a certain configuration of the photosensitive surface of the photodetector and the location of the contacts. Note that the technology applied by us differs significantly from the previously presented one, where the growth of the CdTe crystal film on the InSb substrate results to the formation of an incoherent interface, which hampers the producing of the high-quality heterojunction. The compounds formed at the interface were identified as In_2Te_3 [6] or the stressed phase of InTe [7]. However, the charge transfer mechanism (CTM) in the p-InSb–n-CdTe HJ obtained by us has not yet been studied in detail.

This work is devoted to the study of the CTM in the p-InSb–n-CdTe HJ based on the study of the current-voltage characteristics of the structure at nitrogen temperature, taking into account the features of band discontinuity and bending in the HJ, which results in the appearance of an inversion layer near the interface.

2. EXPERIMENT AND MEASUREMENT RESULTS

To manufacture the p-InSb–n-CdTe HJ, we used the pulsed laser deposition method, which provides the epitaxial growth of CdTe films on InSb plates at rather low substrate temperatures (T_s = 240–250°C), which makes almost impossible the mutual diffusion of semiconductor components. The CdTe films with the thickness of 500 nm are deposited on a polished p-InSb substrate (with the thickness of 500 μm; the acceptor concentration is equal to $N_A = 4.17\times10^{14}$ cm^{-3}). Owing to the proximity of the constant lattices (the mismatch is less than 0.03%) and the thermal expansion coefficients, it is expected that the grown heterojunction will be close to ideal. Measuring the thickness by the MITUTOYO SURFTEST SJ-410 profilometer and investigating the crystal structure of the film by the electron diffraction method on the EMR-100M electron diffraction scanner, we have established the optimal technological conditions to obtain crystalline films. The intensity of the evaporating laser radiation on a CdTe target was 2×10^8 W/cm^2, the thickness of the deposited layer per one evaporating pulse was 2.7 nm, the preferred orientation of the CdTe film is (110), at which the thickness of the CdTe film at the edges is differing from the middle section by 10% (the area is equal to 0.8×0.8 cm^2). The morphology of the CdTe layers was studied on the scanning electron microscope VEGA TS 5130MM, which confirms the tight packing of the film and its non-porousness. Next, a metallic contact is obtained on the CdTe film (the contact diameter is about 0.3 mm) by thermal deposition of indium. By thermally deposition, the backside of the substrate was also entirely covered with indium, which forms a good ohmic contact. At the KEITHLEY-6430 device and at the temperature of 78 K, the dark current-voltage characteristic (CVC) of the p-InSb–n-CdTe HJ, shown in Fig. 1, was investigated.

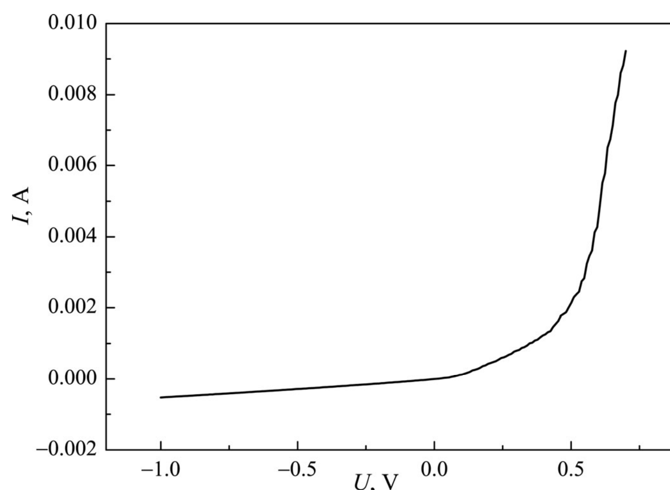

Fig. 1. The forward CVC of the p-InSb–n-CdTe heterojunction.

For the convenience of CTM analysis through the HJ and in order to establish the dominant mechanisms, the direct CVC branches were constructed on a semi-logarithmic (Fig. 2a) and double logarithmic scales (Fig. 2b).

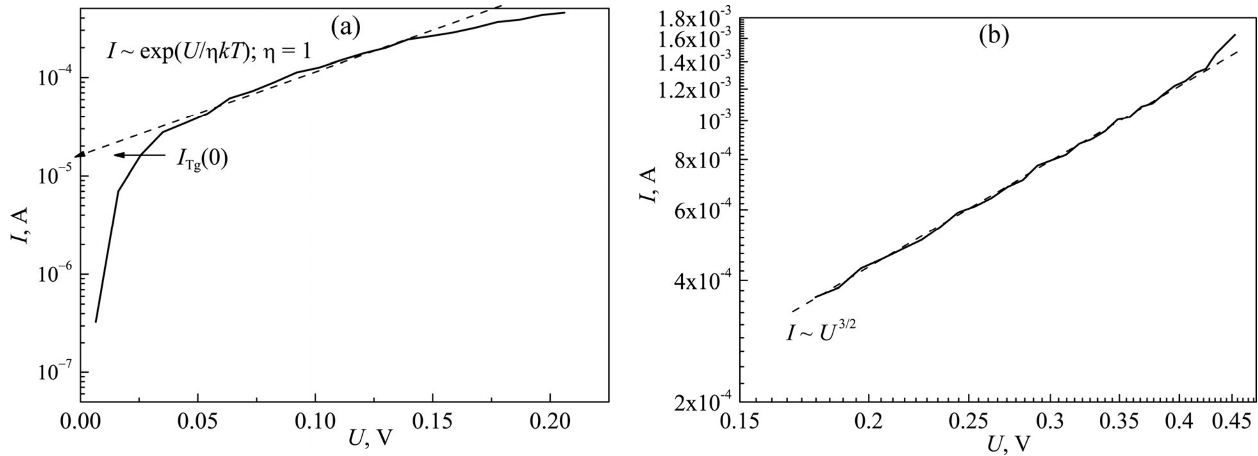

Fig. 2. The direct branch of CVC of the p-InSb–n-CdTe heterojunction.

These graphs show the presence of two dominant CTMs through the HJ. With relatively small bias voltages (0.03 V < U < 0.15 V) the current is satisfactorily consistent with the expression $I \sim \exp(eU/\eta kT)$, where the ideality coefficient is $\eta = 1$ (Fig. 2a). In the region of voltages 0.18 B < U < 0.42 B the CVC obeys the law $I \sim U^{3/2}$. At U > 0.45 V direct current is linearly dependent on the voltage by law $I = (U - U_0)/R_0$, where $U_0 = 0.47$ V is the cut-off voltage of current, and $R_0 = 23\ \Omega$ is the residual differential junction resistance.

The next section presents the model of current flow, describing the CVC, and based on the ideal p-InSb–n-CdTe heterojunction band diagram given in our previous work [3] (Fig. 3).

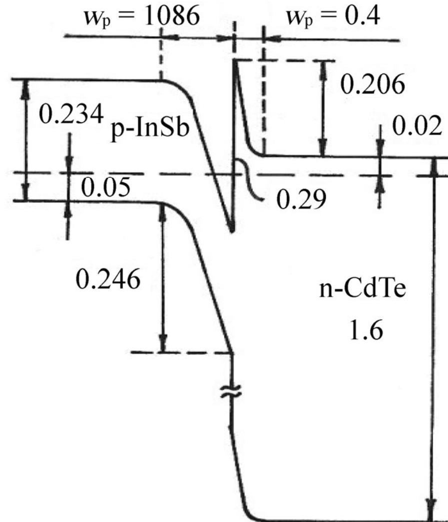

Fig. 3. The band diagram of the p-InSb–n-CdTe heterojunction.

3. THE MODEL OF ELECTRIC CURRENT FLOW

At the formation of the p-InSb–n-CdTe heterojunction, a layer with inverse conductivity is formed near the interface due to the large contact potential difference and rupture of zones in a narrow-gap semiconductor (Fig. 3). Moreover, in p-InSb, where, in addition to the layer of complete depletion (with the width w_p) with the surface density of the negative space charge of the acceptors Q_A, there is also a

charge of free electrons Q_n localized at a certain average distance from the interface. This total negative charge is compensated by the positive charge of the donors Q_D in the n-CdTe layer of complete depletion, having a width w_n. Because there is a gap of more than 1 eV in the valence band, the component of the transition current due to the injection of holes in n-CdTe can be neglected. The transition current at the forward bias will be caused by the injection of electrons into the quasi-neutral InSb region and their subsequent diffusion and recombination with holes. However, here we must bear in mind that, in general, electrons can be injected from two 'reservoirs': from the wide-gap region of n-CdTe and from the well of the inversion layer. In general, the contributions of these reservoirs to the transition current are different, because they differ from each other not only by the concentration of electrons, but also by the height of the barrier, by overcoming which the electrons can be injected into the quasi-neutral part of the InSb. As follows from Fig. 3, in equilibrium the barrier height for above-barrier injection of electrons from n-CdTe is about 0.2 eV, while for electrons localized in the well of the inversion layer, the depth of the well is greater and amounts to 0.25 eV. At small forward biases in the formation of the transition current, first, will give the electrons injected from n-CdTe, a significant part of which without thermalization and trapping into the well, can reach the edge of the space charge region (SCR) in the p-InSb and the increasing of the concentration of minority carriers will create a part of the diffusion transition current. Secondly, due to the decrease in the depth of the inversion well, the additional injection of electrons into the quasi-neutral p-InSb region can also start from it, contributing to the growth of the total HJ current. However, it is necessary to note here that unlike the n-CdTe quasi-neutral region, the concentration of electrons in the inversion layer is not constant, and depends on the band bending in the p-InSb and decreases with the forward bias increase. In addition, if we consider that the charge of electrons concentrated in the inversion layer, in turn, influences the distribution of the external bias between the HJ components, it becomes clear that the formation of the current-voltage characteristic of such heterojunction is a complicated process. Its specific type depends on many factors related both with each other, and on the magnitude of the external bias. In the experiment, an increase in current is observed like $I \sim U^{\alpha}$ ($\alpha \approx 3/2$). We will show that the current increase can really be described in our model by such a power dependence in a certain range of direct voltages.

In equilibrium, the contact potential difference $\Delta\varphi_K$ can be represented as the sum of diffusion potentials attributable to n- and p-regions: $\Delta\varphi_K = \varphi_{n0} + \varphi_{p0}$. When there is an external offset U, the part of it (U_1) falls into the spatial charge region of the CdTe, and the part (U_2) falls within the spatial charge region of the InSb. Accordingly, both the height of the potential barrier for electrons from CdTe and the depth of the potential well in spatial charge region of the p-InSb decrease. They become equal to ($\varphi_{n0} - U_1$) and ($\varphi_{p0} - U_2$). To find the dependences of the charges of ionized donors Q_D, and acceptors Q_A in the spatial charge region, and electrons in the inversion layer Q_n under strong inversion conditions, it is necessary to solve the Poisson equation taking into account the contribution of all these charges [8]. Then the electroneutrality equation for the transition $Q_n + Q_A = Q_D$ can be represented in the form:

$$\sqrt{\frac{\varepsilon_0\varepsilon_2 kT N_A}{2}}\exp\left[\frac{q(\phi_{p0}-2\phi_0-U_2)}{kT}\right]+\sqrt{2q\varepsilon_0\varepsilon_2 N_A(2\phi_0-\frac{kT}{q})}$$
$$=\sqrt{2\varepsilon_0\varepsilon_1 N_D\, q(\Delta\phi_k-\phi_{p0}-U_1)} \tag{1}$$

where ε_1, ε_2 are the dielectric constants of semiconductors CdTe and InSb, ε_0 is the electric constant, q is the elementary charge, $q\varphi_0$ is the energy distance between the middle of the forbidden band and the Fermi

level in the volume of the p-InSb. This equation allows one to find the distribution of external voltage between the spatial charge region of the CdTe and InSb. Here we took into account the fact that the charge of ionized acceptors (the second term in the right-hand side of (1)) does not depend on the potential of the interface and is given by the bending of the zones at the moment of the beginning of a strong inversion in the presence of an electronic inversion layer.

Taking into account the contributions to the current of electrons injected from both the n-CdTe and the inversion well, the transition current density can be represented in the form:

$$j = \frac{qD_n}{L_n}\left[\gamma N_D \exp\left(-\frac{q(\Delta\phi_k - \phi_{po})}{kT}\right)\left(\exp\left(\frac{qU_1}{kT}\right)-1\right) + n(0)\exp\left(-\frac{q\phi_{po}}{kT}\right)\left(\exp\left(\frac{qU_2}{kT}\right)-1\right)\right] \equiv$$
$$\equiv j_0\left[\gamma \exp\left(-\frac{q(\Delta\phi_k - \phi_{po} - 2\phi_0)}{kT}\right)\left(\exp\left(\frac{qU_1}{kT}\right)-1\right) + \xi\left(\exp\left(\frac{qU_2}{kT}\right)-1\right)\right], \quad (2)$$

where γ is the fraction of electrons not-thermalized in the well, D_n, L_n are the coefficient and the length of electron diffusion in the p-InSb, respectively, and $n(0)$ is the volume concentration of electrons in the inversion well, which is given by the magnitude of the band bending and the average electron localization length from the interface λ_c [8]

Parameter	p-InSb	n-CdTe
Band gap width E_g(77K), eV	0.234	1.6
Donor concentration N_D, cm^{-3}	–	1.13×10^{15}
Acceptor concentration N_A, cm^{-3}	4×10^{14}	–
Dielectric constant E	16.8	7.1
Effective density of states in the conduction band N_C(77K), cm^{-3}	–	10^{17}
Effective density of states in the valence band N_V(77K), cm^{-3}	9.45×10^{17}	–
Fermi level position in n-CdTe, eV	-	0.02
Fermi level position in p-InSb, eV	0.05	–
Electronic affinity χ, eV	4.59	4.3
The gap zones in the conduction band ΔE_C, eV	0.29	–
Diffusion length of electron L_n, μm	4.47	–
Electron diffusion coefficient D_n, cm^2/s	2×10^3	–
The lifetime of minority carriers τ_n, s	10^{-10}	–

$$n(0)=\frac{\sqrt{2kT\,\varepsilon_2\varepsilon_0 N_A}}{q\lambda_c}\exp\left(\frac{q(\phi_{p0}-2\phi_0)}{kT}\right). \tag{3}$$

In the numerical computation of the CVC, we use the HJ parameters presented in the Table. Using them and choosing $\gamma = 0.75$ and $\lambda_c = 100$ Å, we obtain $\xi = 0.28$.

The computations show that when significant zone bends remain, and the strong inversion mode continues to take place in the potential well, the external voltage is distributed between the HJ components in proportion $U_1/U_2 \sim 10$ at relatively small external displacements. With increasing voltage this ratio decreases, but still most of the external bias continues be caused by the space charge region of n-CdTe. But, on the other hand, because the concentration of electrons in the inversion well depends exponentially on the bending of the zones, the value of which decreases with the forward bias by U_2, then an accurate estimate of the relative contribution to the total transition current of electrons injected from the CdTe and from the inversion well, described by the first and second terms in expression (2), can only be obtained using a consistent numerical computation.

Figure 4 shows the dependence of the direct current of the HJ on voltage (in dimensionless units) computed based on the formulas obtained above in a double logarithmic scale in the interval of external displacements which is of interest. It can be seen that the current-voltage characteristic of the HJ can indeed be described by the dependence of the type $j \sim U^{\alpha}$, where $\alpha \approx 1.5$.

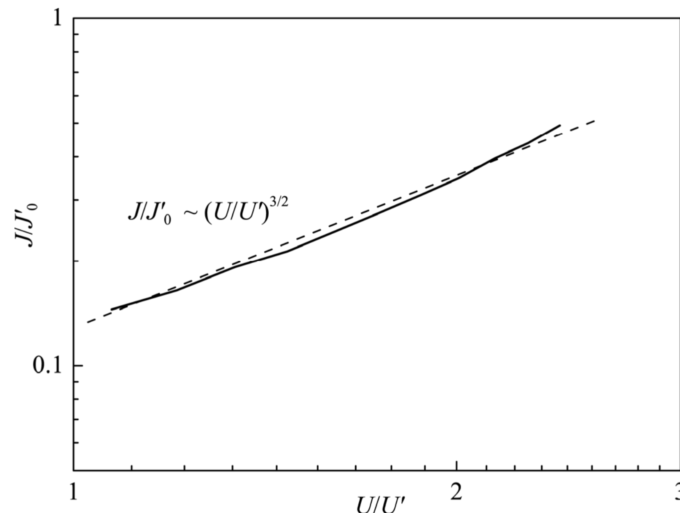

Fig. 4. The theoretical CVC of GP in double logarithmic scale. Here, voltage and current density are presented in relative values ($U_0' = 0.18$ V, $J_0' = 3.6$ mA/cm^2).

4. CONCLUSION

Thus, the work shows that such a feature of the p-InSb–n-CdTe HJ band structure as the presence of an inversion layer in p-InSb near the interface can significantly modify the direct branch of its CVC. In particular, a power-law dependence of current on voltage can be observed in a certain forward bias range similarly to currents limited by a space charge. The presence of the inversion layer should be borne in mind when studying the volt-farad and photovoltaic characteristics of the p-InSb–n-CdTe HJ.

ACKNOWLEDGMENTS

The work was performed in the joint laboratory of the Institute of Radiophysics and Electronics of the National Academy of Sciences of the Republic of Armenia and the Russian-Armenian University with the financial support of the Ministry of Education and Science of the Russian Federation.

REFERENCES

1. Alexanian, A.G., Alexanian, Al.G., Kazarian, R.K., Matevosian, L.A., and Nickogosian. H.S., *J. of Infrared and Millimeter Waves*, 1993, vol. 14, p. 2203.
2. Alexanian, A.G., Aramyan, N.S., Avjyan, K.E., Khachatryan, A.M., Grigoryan, R.P., and Yeremyan, A.S., *Combinatorial and High-Throughput Discovery and Optimization of Catalysts and Materials*, R.A. Potirailo, W.F. Maier (eds.), CRC/Taylor & Francis, 2006.
3. Matevosyan, L.A., Avjyan, K.E., Petrosyan, S.G., and Margaryan, A.V., *Uspekhi Prikladnoi Fiziki*, 2014, vol. 2, p. 403.
4. Hamamatsu technical information, available https://www.hamamatsu.com/us/en/product/index.html
5. Margaryan, A.V., Petrosyan, S.G., Matevosyan, L.A., and Avjyan, K.E., *J. Contemp. Phys*. (*Armenian Ac. Sci*.), 2016, vol. 51, p. 202.
6. Zahn, D.R.T. et al., *Appl. Surf. Sci*., 1989, vol. 41/42, p. 497.
7. van Welzenis. R.G. et al., *Appl. Phys*., 1991, vol. A52, p. 19.
8. Sze, S.M., *Physics of Semiconductor Devices*, Second Edition, vol. 1, John Wiley & Sons Inc., 1981.